Accepted Manuscript

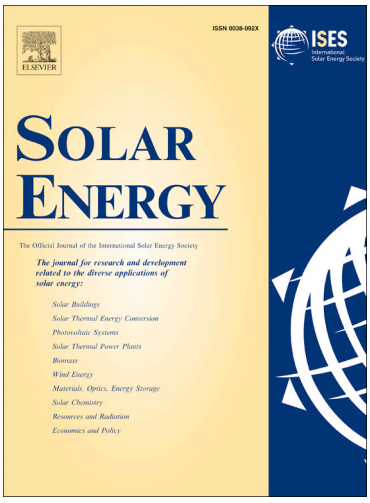

The PV Potential of Vertical Façades: A classic approach using experimental data from Burgos, Spain

M. Díez-Mediavilla, M.C. Rodríguez-Amigo, M.I. Dieste-Velasco, T. García-Calderón, C. Alonso-Tristán

PII: S0038-092X(18)31121-6
DOI: https://doi.org/10.1016/j.solener.2018.11.021
Reference: SE 7394

To appear in: *Solar Energy*

Received Date: 9 June 2018
Revised Date: 14 October 2018
Accepted Date: 8 November 2018

Please cite this article as: Díez-Mediavilla, M., Rodríguez-Amigo, M.C., Dieste-Velasco, M.I., García-Calderón, T., Alonso-Tristán, C., The PV Potential of Vertical Façades: A classic approach using experimental data from Burgos, Spain, *Solar Energy* (2018), doi: https://doi.org/10.1016/j.solener.2018.11.021

The PV Potential of Vertical Façades: a classic approach using experimental data from Burgos, Spain

M. Díez-Mediavilla[a]; M.C. Rodríguez-Amigo[a]; M.I. Dieste-Velasco[a]; T. García-Calderón[a], C. Alonso-Tristán[a*].

[a] Solar and Wind Feasibility Technologies Research Group (SWIFT). Electromechanical Engineering Department. Universidad de Burgos, Spain

*Corresponding author: catristan@ubu.es; cristinaalonso.tristan@ubu.es

Abstract

Potential photovoltaic (PV) production from vertical façades facing the four cardinal points of the compass are calculated from daily average vertical global insolation readings measured in Burgos, Spain. Ten-minute data sets are collected over forty-five months, from January, 2014 to September 2017, in the experimental campaign to produce estimates of daily average insolation levels, from which the PV potential of the vertical surfaces was calculated. Given the scarcity of data on Global Vertical Insolation (GVI), the main sky-related variables were processed in four classic decomposition models (Isotropic, Circumsolar, Klucher, and Hay) to predict the insolation values. Both the experimentally measured GVI values and those calculated with the models were then compared using the statistical indicators RMSE and MBE. The results highlighted the economic viability of Building Integrated PhotoVoltaic (BIPV) facilities, even on the north-facing façades, in comparison with the horizontal facility at the same location.

KEYWORDS: Vertical Global Insolation, BIPV, PV potential, orientation

1. INTRODUCTION

Building Integrated Photovoltaics (BIPV) can be a leading technology in terms of cost and efficiency (Lee et al., 2017). Traditionally, PV have been installed to maximize annual energy production rates. Urban structures, however, are not always optimal for solar energy applications: BIPV system efficiency is affected by such factors as the shading effect due to installation angles and surrounding obstructions, non-optimal orientations, and the temperature increase of PV modules (Lee et al., 2017). Vertical solar panels receive less solar radiation than roofs and horizontal surfaces, particularly in the summer months, and are more affected by the compactness of the urban layout, despite which installations on façades can occupy very large areas. Additionally, vertical PV façades will produce relatively more energy in winter than in the summer months (Hsieh et al., 2013) and in the early and late daylight hours, when the sun is lower in the sky. A building will typically have four, or at least two, façades facing opposite directions, so the maximum energy produced by the solar panels on each building façade will be at a different time of day, distributing the power production peaks throughout the day, and thereby achieving a closer match to the ideal load diagram than would otherwise be the case (Hummon et al., 2013). BIPV offers interesting opportunities in so far as it replaces conventional building materials that can harmoniously complement the architectural design of a building (Brito et al., 2017) and the PV system can contribute significant added merit to buildings in terms of value and image (Montoro et al., 2011).

Data on incident solar radiation and illumination on building surfaces are essential inputs for any simulation of building energy use and for the design of

net zero energy buildings (Wattan and Janjai, 2016), which figure among the main applications of passive solar energy. Moreover, the configuration and the sizing of active solar energy systems need reliable data on incident solar radiation. However, data of incident solar radiation on vertical surfaces are very scarce and have only been recorded at relatively very few locations (Maxwell et al., 1986; Muneer, 1990; Notton et al., 2006; Şaylan et al., 2002; University of Oregon, 2000) and preferentially on south facing facades (Utrillas et al., 1991). The same may also be said of concurrent measurements of horizontal global and horizontal diffuse or direct normal irradiance data.

However, as the measurement of global horizontal irradiance is simple and cost-effective, different methods have been developed that use horizontal data on irradiance to calculate solar irradiance from any orientation on vertical surfaces (Kong and Kim, 2015; Muzathik et al., 2011; Noorian et al., 2008; Pandey and Katiyar, 2011; Wattan and Janjai, 2016). The different physical attributes that are considered in each model (Wattan and Janjai, 2016) produce significant differences in their performance and their results (de Simón-Martín et al., 2017). No universal model has been proposed (Yang, 2016), but the varying conditions of the sky vault should be considered in any review of the isotropic, anisotropic, and circumsolar models.

The main objective of this study is to define the PV potential of vertical façades facing the four (north, south, east and west) cardinal directions, in comparison with horizontal surfaces at the same location. Daily datasets containing Global Horizontal Insolation (GHI), Diffuse Horizontal Insolation (DHI), Beam Horizontal Insolation (BHI) and Vertical Global Insolation (GVI) (Wh/m^2) were recorded over forty-five months in Burgos, Spain. The main contribution of this paper

consists in the extensive experimental measurements resulting in varied data sets that lend support to the viability of vertical BIPV: the joint use of the vertical surfaces oriented in the four cardinal directions receives, annually, twice the insolation obtained on a horizontal surface and tripling the figure in the winter months.

This work proposes the use of transposition models as alternative to obtain GVI data through GHI, BHI and DHI data, magnitudes usually recorded at radiometric facilities. Four empirical models, widely tested in the literature –the Circumsolar (Iqbal, 1983), Klucher (Klucher, 1979), Hay (Hay, 1978), and Isotropic (Iqbal, 1983) models- that considers main sky considerations (isotropic, anisotropic and circumsolar), were used to calculate GVI. Both the experimentally measured GVI values and those calculated with the models were then compared using the statistical indicators RMSE and MBE.

The structure of this study is as follows: the experimental meteorological facility and data used for the study will be described in Section 2. The GVI data will then be presented in Section 3, and the economic viability of the BIPV on new and existing buildings will be discussed, in comparison with a horizontal facility at the same location. The classical decomposition models selected for the calculation of GVI and the justification of the selection will then be presented in Section 4. The experimental and calculated values of GVI calculated with regard to the four cardinal points will be compared in seasonal and multiyear analysis, using the statistical indicators MBE and RMSE. Finally, the main results of the study will be summarized in the Conclusions section.

2. EXPERIMENTAL SECTION

The experimental data for this study were gathered at a meteorological and radiometric facility located on the roof of the Higher Polytechnic School building at Burgos University (42°21′04″N; 3°41′20″O; 856 m above mean sea level). This five-storey building, in an area with no other buildings of comparable height, has a horizon elevation angle that is lower than 10º with regard to the surface where the radiometric station is located. Burgos has an average of 575 mm of precipitation and an average annual global irradiance of 1500 kWh/m^2, as can be seen in a Typical Meteorological Year (TMY) over the last twenty years, compiled by the Spanish State Meteorology Agency (AEMET) (ITACYL-AEMET, 2013). Clear skies are predominant over Burgos (Suárez-García et al., 2018) mainly in spring and summer. The experimental equipment and the geographical location are shown in Figure 1.

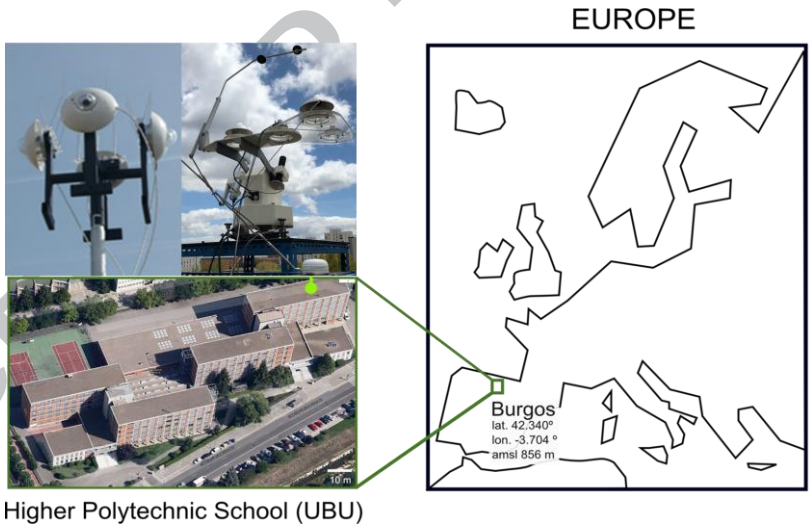

Figure 1. Location of the experimental facility on the roof of the Higher Polytechnic School building at the University of Burgos, Spain.

The facility is equipped with seven pyranometers (Hukseflux/SR11) and a pyrheliometer (Hukseflux/DR01) both for horizontal and tilted measurements and for measurement of the irradiance (W/m^2) from each cardinal orientation. A sun tracker was set to measure Global (GHR), diffuse (DHR), and Beam (BHR)

Horizontal irradiance (W/m^2). Both the pyranometers and the pyrheliometer are classified as “first class” in the ISO classification (ISO 9060:1990) with a WMO performance level that is of “good quality” (WMO-N.08, 7th Ed. 2008) ((WMO), 2010). The calibration and the management of the radiometric facility was done following ISO(1992) and the WMO Guide to Meteorological Instruments and Methods of Observation ((WMO), 2008. (Updated 2010)).

Thirty-second irradiance data (W/m^2) were recorded by a CR3000 Campbell Scientific datalogger from January, 2014 to September 2017. The device has 28 analogic voltage inputs (or 14 differential ones) ranging between ±20 to ±5000 mV and a resolution of between 167µV - 0.67 µV.

The experimental thirty-second data averages of GHR, BHR, DHR, and GVR (North, South, East and West orientations) were recorded every 10 minutes. The ten minutes irradiance data were analysed and filtered using traditional quality criteria (Gueymard and Ruiz-Arias, 2016). Whenever a ten-minute data item failed to match the quality criteria, both the horizontal and the vertical values were eliminated. Cumulative hourly GHI values (Wh/m^2) were calculated from the 10-minute data sets series using the trapezoidal integration. Cumulative daily values were calculated from the hourly data.

Almost 5% of the daily data were eliminated with this procedure. The total amount of daily GHI, BHI, DHI, 4 GVI data used for the study amounted to 1272 daily values in each case.

3. GLOBAL VERTICAL INSOLATION DATA

3.1.- GVI data versus GHI

Daily average solar energy readings from each façade facing each of the cardinal points are presented in Table 1. Daily average GHI is 4.31 ($kWh \cdot m^2$ day^{-1}) and has been used for comparison to the level of incident energy on a vertical facility. The experimental daily average GHI obtained in this work can be compared to the daily average GHI value, 4.36 $kWh \cdot m^{-2} \cdot day^{-1}$, obtained by the Spanish Meteorological Agency (AEMET) (Sancho Ávila et al., 2012) in terms of the daily average insolation on the horizontal plane with data recorded in Burgos, between 1983 and 2005. The levels of GVI measured from the South, the West, and the East orientations received over 50% of the GHI, as shown in Table 1. The value of energy collected from the north-facing façade was close to 30% of the value collected on the horizontal plane.

Table 1. Daily average GVI ($kWh \cdot m^2$ day^{-1}) measured on the façades facing the four cardinal directions (Burgos, Spain) and the ratio with GHI (%)

Insolation	South	East	West	North
GVI ($kWh \cdot m^{-2} \cdot day^{-1}$)	2.99	2.54	2.39	1.23
GVI/GHI (%)	69.4	58.9	55.5	28.3

Monthly distribution of GVI on the façades facing the four cardinal directions and GHI over the year are presented in Table 2. Although the south orientation presented the higher average GVI, the values were lower in May and June (2.79 $kWh \cdot m^{-2} \cdot day^{-1}$) and reached their maximum values in March (3.33 $kWh \cdot m^{-2} \cdot day^{-1}$) and September (3.91 $kWh \cdot m^{-2} \cdot day^{-1}$). The minimum values were obtained in January, with 2.25 $kWh \cdot m^{-2} \cdot day^{-1}$. The east and the west-facing façades presented higher GVI values than the south orientation in summer, reaching 4 $kWh \cdot m^{-2} \cdot day^{-1}$ in July, higher than the values on the south-facing façade over the same month. The GVI on the north-facing façade was

throughout the year, but during the month of June it reached a value 2 kWh·m^{-2}·day^{-1}, as shown in Table 2.

Table 2 shows that a vertical south-facing façade is more efficient between October and January than a horizontal surface. Additionally, the sum of the energy collected from the east and the west-facing façades can equal the value of the south-facing facility. The monthly study of the total energy received by each façade, the sum of the four façades and the GHI values presented in Table 2 show the available energy for a BIPV.

Table 2. Monthly average of daily GVI, GHI and sum of four cardinal orientation GVI (kWh m^{-2} day^{-1})

kWh·m^{-2}·day^{-1}	South GVI	East GVI	West GVI	North GVI	Sum GVI	GHI
January	2.26	0.99	0.99	0.58	4.81	1.69
February	2.43	1.38	1.31	0.79	5.91	2.55
March	3.34	2.44	2.18	1.11	9.07	4.08
April	3.21	3.05	2.93	1.44	10.63	4.96
May	2.82	3.58	3.21	1.85	11.46	6.04
June	2.73	4.08	3.75	2.14	12.70	7.22
July	2.97	4.03	4.00	1.93	12.93	7.42
August	3.50	3.75	3.69	1.55	12.49	6.44
September	3.91	2.97	2.77	1.25	10.91	4.96
October	3.70	1.97	1.88	0.91	8.45	3.05
November	2.45	1.17	1.09	0.63	5.34	1.92
December	2.57	1.02	0.94	0.55	5.07	1.45

The sum of the energy on the vertical facades from the four cardinal directions over the winter months is approximately three times the amount of the energy collected by the horizontal surface and twice that of the rest of the year. The energy levels on the vertical façades show that BIPV could make a useful

contribution to Net Zero Buildings and for distributed energy generation in smart cities.

Individual comparisons of the monthly average of daily GVI versus GHI for all four orientations are presented in Figure 2, and the relative value of GVI/GHI (%) is shown in Table 3.

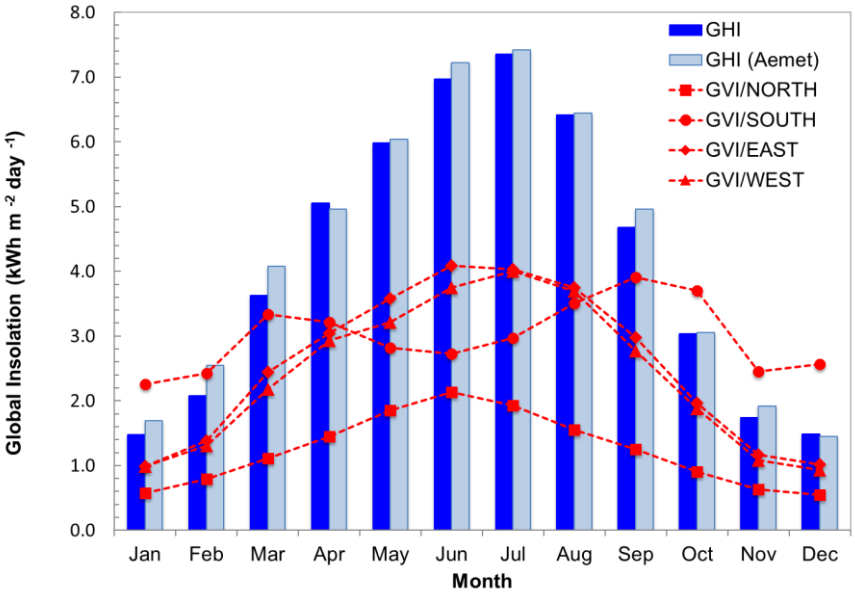

Figure 2. Monthly average GVI and GHI measured in Burgos from all four cardinal directions: a) South; b) East; c) West; d) North.

From Table 3 we see that the south-facing façade only exceeded the horizontal surface in autumn and winter (October to January). During these months, the solar altitude is lower than the rest of the year, so the solar incidence on the south- facing vertical surface is higher than the received by the horizontal one in the same location. In summer, the solar altitude is higher and the incidence on the vertical surface is lower.

The east and west-facing façades present very similar values for energy collected throughout the year, representing almost half of the energy produced

on the horizontal surface. East and west facing surfaces receive the solar radiation approximately with the same incident angle through the year, changing only the number of hours of insolation. The north-facing façade collected a third of the energy measured on the horizontal surface, at most, and less in summer time. No direct insolation receives the north-facing façade in winter and it receives very few hours in summer, only at sunrise and sunset time.

Table 3. Relative value of GVI/GHI (%) measured on each façade

	GVI/GHI (%)			
Month	South	East	West	North
January	133.5	58.3	58.6	34.2
February	95.1	54.2	51.4	31.0
March	81.8	59.8	53.4	27.2
April	64.7	61.4	59.1	29.1
May	46.6	59.2	53.1	30.7
June	37.8	56.6	51.9	29.6
July	40.0	54.4	53.9	26.0
August	54.4	58.2	57.3	24.1
September	78.8	60.0	55.8	25.3
October	121.4	64.4	61.6	29.7
November	127.6	60.9	56.6	33.0
December	177.2	70.1	64.6	38.1

3.2. Economic Study

Prices for PV systems vary widely and depend on a variety of factors including: system size, location, customer type, connection to an electricity grid, technical specifications… and the extent to which end-user prices reflect the real costs of all the components. The International Energy Agency (IEA, 2017b) reported the range of system prices in the global PV in 2016. In Spain, the average price of a

grid-connected residential PV facility is 1.5 €/W. Using standard modules (mono-Si of 180 W_p that occupies 1.28 m^2surface), a conversion factor of $7.1 \cdot 10^{-3}$ m^2/W has been established.

The PV potential is determined by multiplying insolation (I) by an efficiency factor (η_{ref}) of 15% and for a typical module (Hsieh et al., 2013) and a performance ratio (PR) of 80%(Degli Uberti et al., 2010). The performance ratio is a measure of the quality of a PV plant and describes the relationship between the actual and theoretical energy outputs of the PV plant. Environmental factors such as temperature of the PV module, solar insolation and power dissipation or shading of the panels, as well technical factors (panel and inverter efficiency or conduction losses) have influence on the PR value.

Following IEA criteria (IEA, 2017a) and assuming installation cost of the PV facility of 210 €/m^2 and a market price of 0.13 €/kWh (Brito et al., 2017), the payback is calculated as:

$$Payback\ [years] = \frac{210[€/m^2]}{I[kWh \cdot m^{-2} \cdot year^{-1}] \times \eta_{ref} \times PR \times 0.13[€ \cdot kWh^{-1}]} \quad \textit{Eq. 1},$$

where, I is global insolation over the surface; η_{ref} represents the module efficiency; and, PR, the Performance Ratio.

Table 4 shows the estimated payback time for vertical PV facilities in this location. As can be seen a vertical south-facing façade needs only two years more than a horizontal facility to cover its costs at this specific location, while the vertical east and west-facing facilities need a further six years. The competitiveness of a PV system is linked to the location, the technology, the cost of capital, and the cost of the PV system itself that to a large extent

depends on the nature of the installation and its size. The decline in prices observed over the past few years are opening new business models for PV deployment, even if very low prices will not always imply competitive alternatives in every sense (IEA, 2017b).

Table 4. Financial payback time of investment for a horizontal surface and vertical façade at Burgos, Spain.

System	Insolation ($kWh \cdot m^{-2}$ $year^{-1}$)	Payback (years)
Horizontal facility	1400	10
North-facing façade	450	30
South-facing façade	1091	12
East-facing façade	927	15
West-facing façade	872	15

4. GVI VALUES FROM GHI: A CLASSIC APROACH

4.1. Selection of classic decomposition models.

Several studies have been performed to arrive at irradiance solar values at different tilts and orientations and there are many experimental and theoretical models proposed for this purpose. The majority of these works determine which model best fits in the area under study or which angle of inclination or orientation best optimizes the irradiance value (Evseev and Kudish, 2009; Khalil and Shaffie, 2016; Kong and Kim, 2015; Mehleri et al., 2010; Muzathik et al., 2011; Noorian et al., 2008). The diffuse component of irradiance is a component in some studies that offers various different approaches to sky anisotropy (Gueymard, 1987; Li and Lam, 2000; Li et al., 2002; Pandey and Katiyar, 2011; Raptis et al., 2017; Wattan and Janjai, 2016). Quantification of model uncertainty and the influence of the parameters used to simulate the behaviour

of the facilities with regard to such uncertainty are other goals of the studies that have been reviewed (Xie and Sengupta, 2016). The influence of (clear, cloudy, or partially cloudy) sky conditions on the value of GVI was also studied (Li and Lam, 2004). A complete review of the methodologies to obtain global insolation data over tilted surfaces was established based on nine criteria, using GHI values and different geometric and solar parameters (Gueymard and Myers, 2008). Twenty-six models at four different locations were tested in (Yang et al., 2013) and the results of the pairwise Diebold-Mariano test showed that that no universal model could be conclusively defined.

Having reviewed the literature, four classic models were selected to obtain the GVI data that would be the main input to calculate the PV potential of the vertical façades in all four cardinal directions. The goodness of all the models is strongly dependent on atmospheric factors (Wattan and Janjai, 2016). The selected models are referenced in most reviews and has been tested in different locations around the world (Kong and Kim, 2015), (Orehounig et al., 2014), (Khalil and Shaffie, 2013), (Gueymard, 1987) (Demain et al., 2013). Their main advantage is that they only require for their application the direct, diffuse and global components on a horizontal plane, magnitudes usually measured in radiometric facilities. All possible sky conditions were taken into account: clear, overcast and partially cloudy skies. The Circumsolar model (Iqbal, 1983) refers to clear skies. The Isotropic model (Iqbal, 1983) was specifically developed for uniformly covered sky and the Hay (Hay, 1978) and the Klucher (Klucher, 1979) models are anisotropic models with different approaches to overcast skies: Klucher adds cloud sky conditions to the clear

sky model and the Hay model adds a circumsolar solar component to the isotropic conditions of the sky vault.

Classic decomposition models assume that global solar insolation is the sum of three factors: beam, ground-reflection, and sky-diffusion. Each model features a different mathematical expression for calculating these components. The classic models selected for this study are used to calculate global insolation on tilted surfaces. When the selected tilt angle is $\frac{\pi}{2}$, the calculated magnitude is GVI. The input data are GHI, BHI and DHI. A south-facing tilt angle is usually considered, but in this study, north, west and east oriented planes are also studied.

Hourly global insolation incident on an inclined plane, β, facing a given direction, γ, is calculated as:

$$I_{\beta\gamma} = I_{b\beta\gamma} + I_{d\beta} + I_r \qquad \textit{Eq. 2,}$$

where, $I_{b\beta\gamma}$ is the hourly beam insolation incident on an inclined surface, β, and oriented in direction γ; $I_{d\beta}$ is the hourly diffuse insolation incident on an inclined surface, β, facing any given direction; and, I_r is the hourly ground-reflected diffuse insolation incident on an inclined surface. In our work, $\beta = \frac{\pi}{2}$, and γ adopts the values of $0, \pi, \frac{\pi}{2}$ or $-\frac{\pi}{2}$, for the south, north, east and west facing façade, respectively.

$$I_{b\beta\gamma} = I_b . r_b \qquad \textit{Eq. 3.}$$

Equation 2 was used to calculate the hourly beam insolation where, I_b is the hourly horizontal beam insolation, and r_b is the ratio of the hourly extra-

terrestrial insolation on a randomly tilted plane in relation to the horizontal, given by

$$r_b = \frac{cos\theta}{cos\theta_z} \qquad \textit{Eq. 4.}$$

θ is the angle between beam insolation and surface normal, for a surface inclined in any arbitrary direction; and, θ_z is the zenith angle or the angle between the beam from the sun and the vertical.

For the calculation of the third term in Eq. 2, the hourly ground-reflected insolation, two different cases can be considered. The case of isotropic reflection, is calculated using the Eq. 5, and the case of anisotropic reflection, uses the Eq.6:

$$I_r = \frac{1}{2} I\rho(1 - cos\beta) \qquad \textit{Eq. 5,}$$

$$I_r = \frac{1}{2} I\rho(1 - cos\beta)\left[1 + sin^2\left(\frac{\theta_z}{2}\right)\right](|cos\Delta|) \qquad \textit{Eq. 6,}$$

where, I is the hourly global insolation incident on a horizontal surface; ρ is the ground albedo; and, Δ is the azimuth of the tilted surface with respect to that of the sun.

The four models differ with regard to the equations they use to calculate the diffuse component of global insolation, $I_{d\beta}$, as described below:

a) Isotropic model:

$$I_{d\beta} = \frac{1}{2} I_d(1 + cos\beta) \qquad \textit{Eq. 7.}$$

b) Circumsolar:

$$I_{d\beta} = I_d . r_b \qquad \textit{Eq. 8.}$$

c) Klucher:

$$I_{d\beta} = \frac{1}{2} I_d (1 + cos\beta) \left[1 + Fsin^3\left(\frac{\beta}{2}\right)\right](1 + Fcos^2\theta . sin^3\theta_z) \qquad \textit{Eq. 9.}$$

d) Hay:

$$I_{d\beta} = I_d \left\{\frac{I - I_d}{I_0} r_b + \frac{1}{2}(1 + cos\beta)\left[1 - \frac{I - I_d}{I_0}\right]\right\} \qquad \textit{Eq. 10,}$$

where, I_d is the hourly diffuse insolation incident on a horizontal surface; I_0 is the extra-terrestrial hourly insolation incident on a horizontal surface; and, F is a modulating function given by: $F = 1 - \left(\frac{I_d}{I}\right)^2$.

Two classic statistical indicators were used to estimate the goodness of the models, RMSE (Root-Mean-Square Error) and MBE (Mean Bias Error), defined as follows:

$$RMSE = \frac{\sqrt{\frac{\sum (V_e - V_t)^2}{N}}}{\langle V_e \rangle} 100 \qquad \textit{Eq. 11.}$$

$$MBE = \frac{\frac{\sum (V_e - V_t)}{N}}{\langle V_e \rangle} 100 \qquad \textit{Eq. 12,}$$

where, V_e are the experimental daily values of GVI (kWh·m^{-2}·day^{-1}); V_t are the calculated daily values of GVI; N is the number of data for the study; and, $\langle V_e \rangle$ is the average of the experimental values of daily GVI.

4.2. Results

The daily values of GVI in the four orientations were calculated with the four models, using the experimental average daily data on GHI, BHI, and DHI as the input for the models. The calculated values were compared with the experimental ones and the statistical indicators, RMSE (Eq. 11) and MBE (Eq. 12), were calculated for each model. Table 5 shows the results of the RMSE and MBE (%) calculated for each orientation and model.

Table 5. Statistical indicators MBE and RMSE (%) calculated from eq. 11 and 12 comparing the experimental and the calculated values of GVI ($Wh \cdot m^{-2} \cdot day^{-1}$) for each orientation and model.

%	South		East		West		North	
Model	RMSE	MBE	RMSE	MBE	RMSE	MBE	RMSE	MBE
Isotropic	80.1	60.6	74.0	55.0	71.4	52.5	25.1	7.1
Circumsolar	41.8	4.9	25.0	3.1	23.6	-2.4	121.0	91.6
Klucher	15.8	-7.2	23.9	7.3	25.5	13.3	24.9	7.0
Hay	21.12	-12.19	21.99	0.51	22.97	6.18	41.53	-26.80

All the models in Table 5 present high values for both statistical indicators, RMSE and MBE. With regard to RMSE, the best fit was achieved with the Klucher model on the south oriented vertical surface, the Hay model on the west and the east-facing surfaces and the Isotropic model for the north-oriented vertical façades.

The Circumsolar model presented the highest deviation in the calculation of GVI on the north-facing façade (>100%). As this is a clear sky model, the diffuse fraction is nearly zero for this model. The diffuse component of the north orientation provided practically 100% of the incident energy (Pérez-Burgos et al., 2010). The Isotropic model showed the highest error (>70%) in the other orientations. This model represents a uniformly cloud sky, a sky type that is not very common in Burgos (Suárez-García et al., 2018). However, the results of the model showed a close fit with the GVI calculated on the north-facing façade, due to the diffuseness of the insolation from that direction. In contrast, the Klucher and the Hay anisotropic models presented comparable results for both the east and the west orientations. The Klucher model showed slightly better

predictions when compared with the results from the north and the south-facing façades and likewise, the Hay model, on the east and the west-facing vertical façades. These results are in agreement with those presented in the literature (Khalil and Shaffie, 2013; Pérez-Lombard et al., 2008; Raptis et al., 2017).

The MBE indicator (See Table 5) showed that the Isotropic model overestimated the calculated value of GVI in all orientations, as well the Circumsolar model, except for the west-facing orientations. Both the Klucher and the Hay model underestimated the calculated value of GVI for the south orientation and both models calculated higher values of GVI for the east and the west-facing façades. On the north-facing façade, the Klucher models overestimated the recorded values and the Hay model underestimated them.

A multi-year analysis of the results was completed, due to the seasonal nature of solar insolation. This study shows the homogeneity of GVI data along the measurement campaign since none of the studied years differs significantly. RMSE (%) values obtained from the application of the four models over the four years under study and for all the oriented surfaces are presented in Figure 3. The two indicators in this study, RMSE and MBE, showed very similar patterns over the years. Both the Klucher and the Hay models presented RMSE values ranging between 31% and 44% (North orientation, 2016) to 14% and 18% (South orientation, 2014), respectively. Both models showed worse behaviour for the north orientation in 2016. The remaining models showed no matches for the orientations with the best and the worst behaviour: the Isotropic model had the lowest RMSE for the north orientation in 2017, while the Circumsolar model presented its best result for the west orientation in 2017. The Circumsolar

model stood out with the highest values of RMSE for the north-facing orientation.

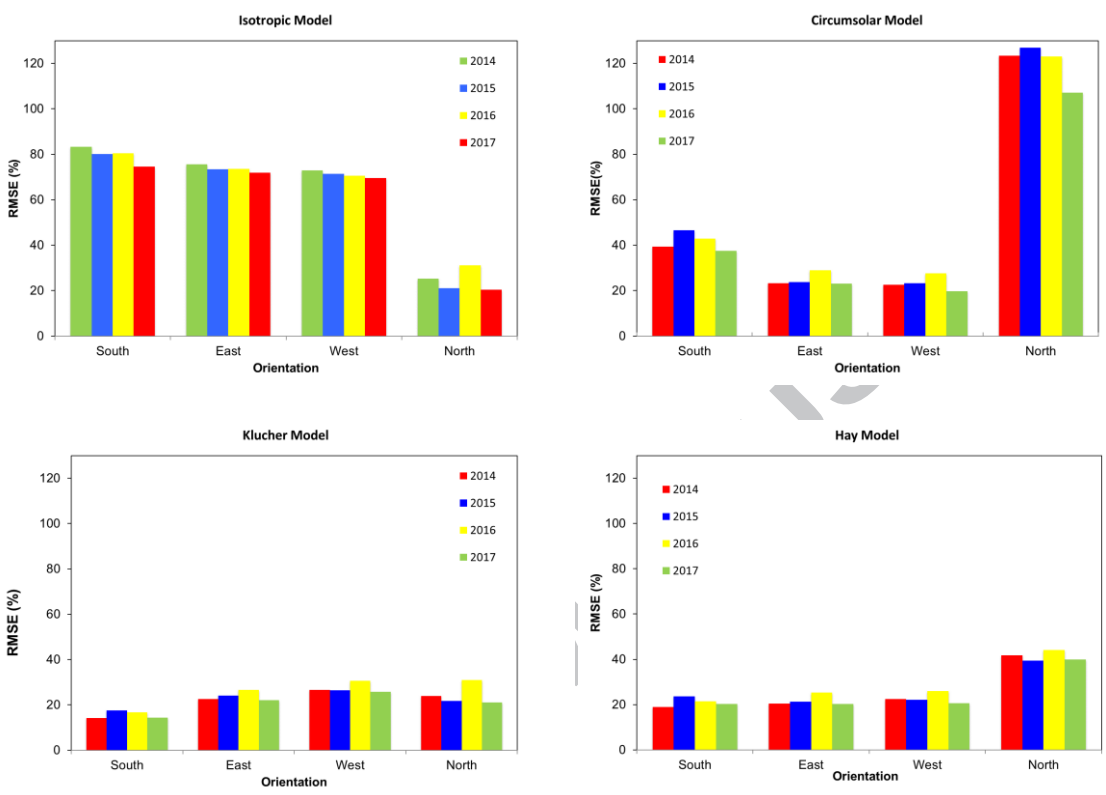

Figure 3. Multi-year analysis (2014-2017) of RMSE values (%) of predicted GVI from the four cardinal directions calculated with the four classic models: Isotropic, Circumsolar, Klucher, and Hay.

A seasonal study was also performed to classify the predicted insolation by month of the year. Throughout the year, all the models presented the highest deviation in the calculation of north-oriented GVI. Figure 4 shows the monthly distribution of RMSE calculated from the four models of both the north (Figure 4-a) and south-facing (Figure 4-b) façades. The results of the Isotropic model fit with an average RMSE of 23% for the north orientation throughout the year. The Circumsolar model was not applied in the winter months at the north façade (from October to February), because the solar angle at this orientation was less than 90º. This model largely failed the rest of the year with RMSE values higher

than 80%. The Hay model had slightly higher RMSE values than the Isotropic model.

Figure 4-b shows the behaviour of the models in the south-facing façade. The Isotropic model presented the worst fit with the experimental data results in the winter months, with RMSE values higher than 100%, decreasing in autumn and spring and reaching 43% in summer time. The Circumsolar model showed an RMSE of around 60% in winter for that same orientation, while these values were slightly lower (around 50%) in summer, and the minimum values (21%) were in autumn and spring. Both the Klucher and the Hay model showed the lowest RMSE values for this orientation throughout the year, ranging from 27% in August to almost 11% in October.

All the models presented similar results for the east and the west orientations, with RMSE values close to 70% for the Circumsolar model and lower for the Hay and the Klucher models, respectively.

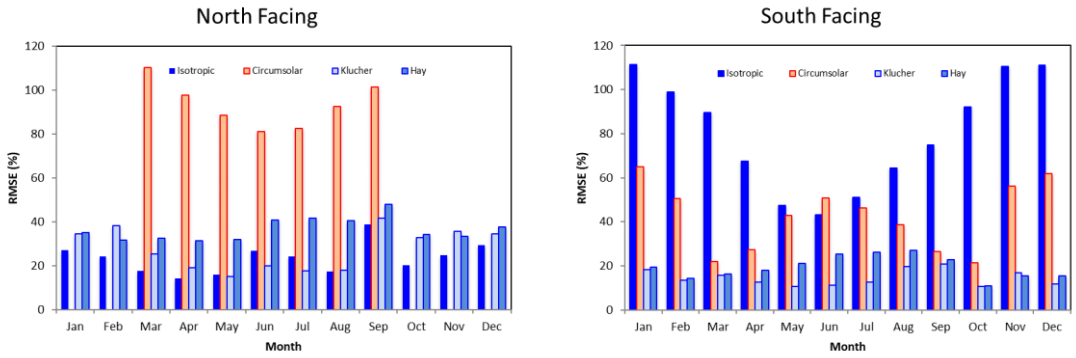

(a) (b)

Figure 4. RMSE (%) of the fitting of the experimental GVI data with the predictions of the four classic models (Isotropic, Circumsolar, Klucher and Hay) for a North-facing façade, and b) for a south-facing façade.

The anisotropic models showed high errors in the north orientation; the Klucher and the Hay models showed similar behaviour, and the Isotropic models presented the highest deviation. The results obtained in this work are in agreement with those presented in the literature (Khalil and Shaffie, 2013; Pérez-Lombard et al., 2008; Raptis et al., 2017). All models have demonstrated better fitting for the calculation of GVI on south-facing rather than north-facing surfaces. The Klucher model made acceptable predictions in relation to the south-facing surfaces, and presents the best result for the north facing surfaces. For the west and east facing surfaces, Hay, Klucher and Circumsolar models got very close result of RMSE.

5. CONCLUSIONS

Forty-five months of daily insolation data over horizontal surfaces and vertical façades facing the four cardinal points of the compass have been measured and analysed in the city of Burgos, Spain. The average solar energy measured in all vertical orientations would be suitable to achieve the energetic and the economic viability of BIPV facilities, taking into account the current price of PV modules and the electricity that the modules could generate.

The south-facing façade received an average daily insolation of 2.99 kWh/m^2 day. The average daily insolation measurements over both the east and the west-facing façades in this study were 2.54 and 2.39 kWh/m^2 per day, while the north orientation received only 1.23 kWh/m^2 per day. These values represented 69.37%, 58.93%, 55.45%, and 28.53% of the received solar energy over the horizontal plane located at the same location.

It is remarkable that the sum of the energy collected by the four vertical façades facing all cardinal points represented almost twice the total energy collected from a horizontal surface at the same location over the year. This same sum in winter time was almost three times greater. These observations underline the suitability of all vertical surfaces for the installation of PV facilities, which would produce relatively high energy values in seasons in which the production on the horizontal plane is low. In winter time, the energy collected from a south-facing façade would be even higher than the energy over the horizontal plane. It is important to notice that the PV potential estimated in this work is for flat facades completely exposed to solar radiation, without shadows or balconies.

The results of the four classic decomposition models applied to calculate GVI, through GHI, BHI, and DHI, have been considered acceptable, on the basis of a relatively low RMSE, when estimating daily average GVI. The Klucher model was the most suitable model for all orientations, while the Isotropic model was only valid for the north orientation, and the Circumsolar model for the east and the west-facing surfaces. The characteristics of the local sky must also be taken into account when choosing the model that will estimate the GVI value from the available GHI, BHI, and DHI data.

Building Integrated PV (BIPV) is seen as one of the five major tracks for effective market penetration of PV. It will contribute to the ambitious aim of zero energy buildings in the built environment. BIPV is increasingly seen as a means of producing electricity locally rather than buying it from the grid. As has been noted, the values of solar insolation available over vertical surfaces are sufficiently high to guarantee the energetic and economic viability of BIPV

facilities showing average payback times for all four cardinal directions of approximately 18 years.

6. ACKNOWLEDGMENTS AND FUNDING

The authors gratefully acknowledge financial support from the Regional Government of Castile and Leon (*Junta de Castilla-León*) (Ref. BU034U16) through the European Regional Development Fund, and from the Spanish Ministry of Economy, Industry and Competitiveness, under the I+D+i State Programme Challenges for Society (Ref. ENE-2014-54601-R).

7. BIBLIOGRAPHY

(WMO), W.M.O., 2008. (Updated 2010). Guide to Meteorological Instruments and Methods of Observation. N0.8.

(WMO), W.M.O., 2010. Technical Regulations. Volume I: General Meteorological Standards and Recommended Practise. Available from: http://library.wmo.int/pmb_ged/wmo_49-vl-2012_en.pdf.

Brito, M.C., Freitas, S., Guimarães, S., Catita, C., Redweik, P., 2017. The importance of facades for the solar PV potential of a Mediterranean city using LiDAR data. Renewable Energy 111, 85-94

de Simón-Martín, M., Alonso-Tristán, C., Díez-Mediavilla, M., 2017. Diffuse solar irradiance estimation on building's façades: Review, classification and benchmarking of 30 models under all sky conditions. Renewable and Sustainable Energy Reviews 77, 783-802

Degli Uberti, F., Faranda, R., Leva, S., Ogliari, E., 2010. Performance Ratio of a PV power plant: different panel technologies comparison, Proc. Solar Energy Tech Workshop, Vol 8, 13-24.

Demain, C., Journée, M., Bertrand, C., 2013. Evaluation of different models to estimate the global solar radiation on inclined surfaces. Renewable Energy 50, 710-721

Evseev, E.G., Kudish, A.I., 2009. An assessment of a revised Olmo et al. model to predict solar global radiation on a tilted surface at Beer Sheva, Israel. Renewable Energy 34(1), 112-119

Gueymard, C., 1987. An anisotropic solar irradiance model for tilted surfaces and its comparison with selected engineering algorithms. Solar Energy 38(5), 367-386

Gueymard, C.A., Myers, D.R., 2008. Validation and ranking methodologies for solar radiation models, Modeling solar radiation at the earth's surface. Springer, pp. 479-510.

Gueymard, C.A., Ruiz-Arias, J.A., 2016. Extensive worldwide validation and climate sensitivity analysis of direct irradiance predictions from 1-min global irradiance. Solar Energy 128, 1-30

Hay, J.E., 1978. Calculation of the Solar Radiation Incident on Inclined Surfaces, Proceedings first Canadian Solar Radiation Data Workshop, Toronto. Ontario, Canada 1978.

Hsieh, C.M., Chen, Y.A., Tan, H., Lo, P.F., 2013. Potential for installing photovoltaic systems on vertical and horizontal building surfaces in urban areas. Solar Energy 93, 312-321

Hummon, M., Denholm, P., Margolis, R., 2013. Impact of photovoltaic orientation on its relative economic value in wholesale energy markets. Progress in Photovoltaics: Research and Applications 21(7), 1531-1540

IEA, 2017a. International Energy Agency: Technical Assumptions Used in PV Financial Models Review of Current Practices and Recommendations. Available from: http://www.iea-pvps.org. (Accessed October, 2018).

IEA, 2017b. Trends 2017 in Photovoltaic Applications: Survey Report of Selected IEA Countries between 1992 and 2016. Available from: http://www.iea-pvps.org. (Accessed October, 2018).

Iqbal, M., 1983. An introduction to solar radiation. Academic Press.

ITACYL-AEMET, 2013. Atlas Agroclimático de Castilla y León. Available from: http://atlas.itacyl.es. (Accessed October, 2018).

Khalil, S.A., Shaffie, A.M., 2013. A comparative study of total, direct and diffuse solar irradiance by using different models on horizontal and inclined surfaces for Cairo, Egypt. Renewable and Sustainable Energy Reviews 27, 853-863

Khalil, S.A., Shaffie, A.M., 2016. Evaluation of transposition models of solar irradiance over Egypt. Renewable and Sustainable Energy Reviews 66, 105-119

Klucher, T.M., 1979. Evaluation of models to predict insolation on tilted surfaces. Solar energy 23(2), 111-114

Kong, H.J., Kim, J.T., 2015. Evaluation of global vertical illuminance and irradiance models against data from Yongin, South Korea. Energy and Buildings 91, 139-147

Lee, H.M., Yoon, J.H., Kim, S.C., Shin, U.C., 2017. Operational power performance of south-facing vertical BIPV window system applied in office building. Solar Energy 145, 66-77

Li, D.H., Lam, J.C., 2000. Evaluation of slope irradiance and illuminance models against measured Hong Kong data. Building and Environment 35(6), 501-509

Li, D.H., Lam, J.C., 2004. Predicting solar irradiance on inclined surfaces using sky radiance data. Energy Conversion and Management 45(11-12), 1771-1783

Li, D.H., Lam, J.C., Lau, C.C., 2002. A new approach for predicting vertical global solar irradiance. Renewable Energy 25(4), 591-606

Maxwell, E.L., Stoffel, T.L., Bird, R.E., 1986. Measuring and modeling solar irradiance on vertical surfaces.

Mehleri, E.D., Zervas, P.L., Sarimveis, H., Palyvos, J.A., Markatos, N.C., 2010. Determination of the optimal tilt angle and orientation for solar photovoltaic arrays. Renewable Energy 35(11), 2468-2475

Montoro, D.F., Vanbuggenhout, P., Ciesielska, J., 2011. Building Integrated Photovoltaics: An overview of the existing products and their fields of application. Report Prepared in the Framework of the European Funded Project; SUNRISE: Saskatoon, Canada

Muneer, T., 1990. Solar radiation model for Europe. Building services engineering research and technology 11(4), 153-163

Muzathik, A.M., Ibrahim, M.Z., Samo, K.B., Wan Nik, W.B., 2011. Estimation of global solar irradiation on horizontal and inclined surfaces based on the horizontal measurements. Energy 36(2), 812-818

Noorian, A.M., Moradi, I., Kamali, G.A., 2008. Evaluation of 12 models to estimate hourly diffuse irradiation on inclined surfaces. Renewable Energy 33(6), 1406-1412

Notton, G., Poggi, P., Cristofari, C., 2006. Predicting hourly solar irradiations on inclined surfaces based on the horizontal measurements: Performances of the

association of well-known mathematical models. Energy Conversion and Management 47(13), 1816-1829

Orehounig, K., Dervishi, S., Mahdavi, A., 2014. Computational derivation of irradiance on building surfaces: An empirically-based model comparison. Renewable Energy 71, 185-192

Pandey, C.K., Katiyar, A.K., 2011. A comparative study of solar irradiation models on various inclined surfaces for India. Applied Energy 88(4), 1455-1459

Pérez-Burgos, A., de Miguel, A., Bilbao, J., 2010. Daylight illuminance on horizontal and vertical surfaces for clear skies. Case study of shaded surfaces. Solar Energy 84(1), 137-143

Pérez-Lombard, L., Ortiz, J., Pout, C., 2008. A review on buildings energy consumption information. Energy and Buildings 40(3), 394-398

Raptis, P.I., Kazadzis, S., Psiloglou, B., Kouremeti, N., Kosmopoulos, P., Kazantzidis, A., 2017. Measurements and model simulations of solar radiation at tilted planes, towards the maximization of energy capture. Energy 130, 570-580

Sancho Ávila, J.M., Riesco Martín, J., Jiménez Alonso, C., Sánchez de Cos, M.d.C., Montero Cadalso, J., López Bartolomé, M., 2012. Atlas de Radiación Solar en España utilizando datos del SAF de Clima de EUMETSAT.

Şaylan, L., Şen, O., Toros, H., Arısoy, A., 2002. Solar energy potential for heating and cooling systems in big cities of Turkey. Energy Conversion and Management 43(14), 1829-1837

Suárez-García, A., Granados-López, D., González-Peña, D., Díez-Mediavilla, M., Alonso-Tristán, C., 2018. Seasonal caracterization of CIE standard sky types above Burgos, northwestern Spain. Solar Energy 169, 24-33

University of Oregon. Solar Radiation Monitoring Laboratory, 2000. Available from: http://solardat.uoregon.edu/index.html. (Accessed October, 2018).

Utrillas, M., Martinez-Lozano, J., Casanovas, A., 1991. Evaluation of models for estimating solar irradiation on vertical surfaces at Valencia, Spain. Solar Energy 47(3), 223-229

Wattan, R., Janjai, S., 2016. An investigation of the performance of 14 models for estimating hourly diffuse irradiation on inclined surfaces at tropical sites. Renewable Energy 93, 667-674

Xie, Y., Sengupta, M., 2016. Diagnosing model errors in simulation of solar radiation on inclined surfaces, Photovoltaic Specialists Conference (PVSC), 2016 IEEE 43rd. IEEE, pp. 1022-1025.

Yang, D., 2016. Solar radiation on inclined surfaces: Corrections and benchmarks. Solar Energy 136, 288-302

Yang, D., Dong, Z., Nobre, A., Khoo, Y.S., Jirutitijaroen, P., Walsh, W.M., 2013. Evaluation of transposition and decomposition models for converting global solar irradiance from tilted surface to horizontal in tropical regions. Solar Energy 97, 369-387

Graphical abstract

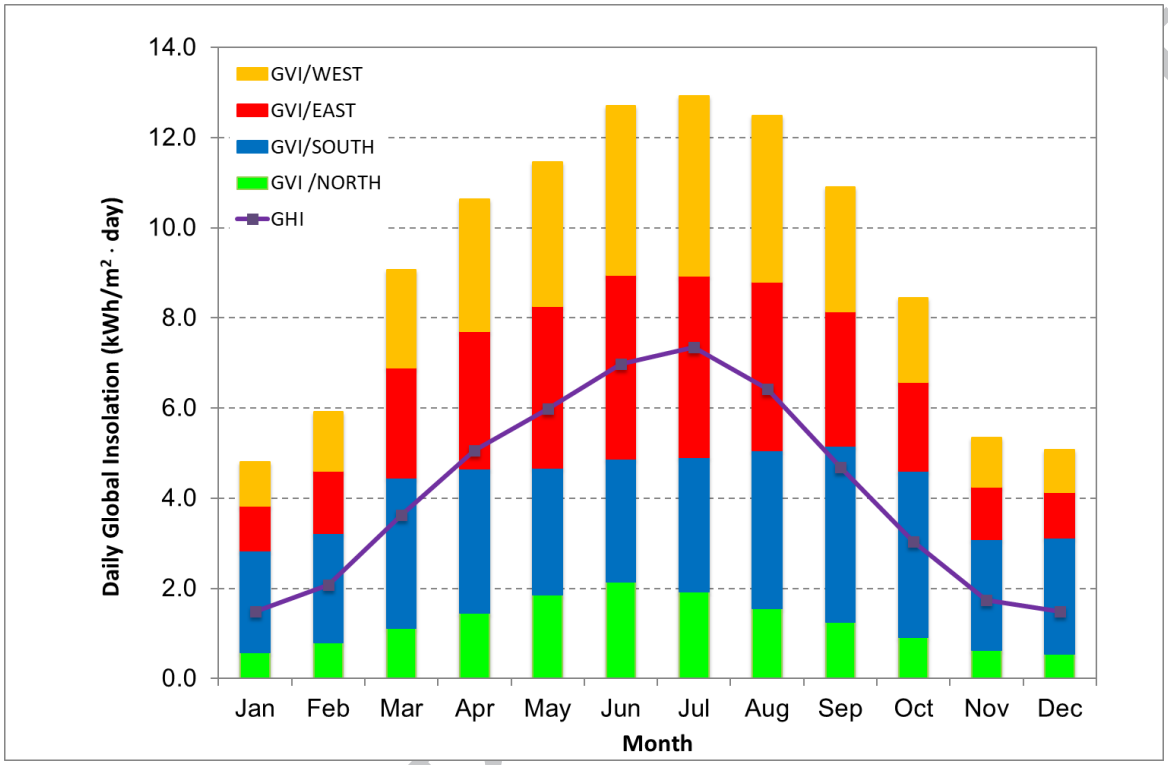

Data recorded in Burgos, Spain, from January, 2014 to September 2017.

Highlights

- Potential PV production from vertical façades are calculated from GVI.
- Data were compared to the energy production of a horizontal facility.
- Four classic decomposition models were tested to predict GVI.
- The results highlighted the economic viability of BIPV.